

# Power Spectrum Analysis of the 2dF QSO Sample Revisited

Kazuhiro Yamamoto

*Graduate School of Science, Hiroshima University, Higashi-Hiroshima, 735-8526, Japan*

kazuhiro@hiroshima-u.ac.jp

## ABSTRACT

We revisit the power spectrum analysis of the complete sample of the two degree field (2dF) QSO redshift (2QZ) survey, as a complementary test of the work by Outram et al. (2003). A power spectrum consistent with that of the 2QZ group is obtained. Differently from their approach, fitting of the power spectrum is investigated incorporating the nonlinear effects, the geometric distortion and the light-cone effect. It is shown that the QSO power spectrum is consistent with the  $\Lambda$  cold dark matter (CDM) model with the matter density parameter  $\Omega_m = 0.2 \sim 0.5$ . Our constraint on the density parameter is rather weaker than that of the 2QZ group. We also show that the constraint slightly depends on the equation of state parameter  $w$  of the dark energy. The constraint on  $w$  from the QSO power spectrum is demonstrated, though it is not very tight.

*Subject headings:* methods: analytical – quasars: general – cosmological parameters – large-scale structure of Universe

## 1. Introduction

The 2dF QSO redshift (2QZ) survey has established that the QSO sample is a useful probe of cosmological models as a tracer of the large scale distribution of mass (Croom, et al. 2001; Hoyle, et al. 2002). In general, constraints on cosmological parameters from QSO sample are not very tight. However, the cosmological parameters estimated from the QSO sample have a unique implication for cosmology (Outram, et al. 2003; Yamamoto 2003a). For example, the cosmological principle can be tested by comparing with the result from other observations such as galaxy redshift survey and cosmic microwave background anisotropies. The pioneering work on the QSO power spectrum analysis was done by Hoyle et al. (2002) with the 2QZ 10000 catalogue. Recently Outram et al. have reported the result of the similar analysis with the final 2QZ catalogue containing 22652 QSOs (2003). They have shown that the QSO power spectrum is consistent with the Hubble Volume

$\Lambda$ CDM simulation. Furthermore, by fitting the power spectrum with the  $\Lambda$ CDM model within linear theory of density perturbations, they obtained a constraint on the cosmological density parameters.

In the modeling of the QSO power spectrum in Outram et al (2003), however, the light-cone effect (Matarrese et al. 1997; Matsubara, Suto & Szapdi 1997; Yamamoto & Suto 1999), the geometric distortion (Ballinger, Peacock & Heavens 1996; Matsubara & Suto 1996) and the nonlinear effects (Mo, Jing & Börner 1997; Magira, Jing & Suto 2000) are not taken into account. The neglect of these effects might fail to estimate the correct cosmological parameters. To test this point, we revisit the power spectrum analysis of the 2QZ sample. We have independently performed the power spectrum analysis of clustering with the complete 2QZ sample. Then we fit the 2QZ power spectrum with theoretical template incorporating the effects, which are not considered in the work by Outram et al. (2003). The methodology in the present paper is almost same as that in the reference (Yamamoto 2002), in which the fitting of the 2dF QSO power spectrum from the 10000 catalogue was investigated using an analytic approach. Thus the primary purpose of the present paper is to test the robustness of the result by Outram et al. (2003) for independent determination of the power spectrum and for more careful modeling of the theoretical power spectrum, including the nonlinear effects, the geometric distortion and the light-cone effect.

On the other hand, Calvao et al. (2002) claimed that the equation of state of the dark energy  $w$  might be constrained from the 2dF QSO sample. Due to the geometric distortion effect, the QSO redshift-space power spectrum may depend on  $w$  even if the original matter power spectrum (or the transfer function) does not depend on  $w$  (Yamamoto 2003b). The strategy in the present paper is not the one proposed by Calvao et al. (2002), however, we check a constraint on  $w$  by considering how the estimated density parameters depends on  $w$  by the fitting of the power spectrum. The second purpose of this paper is to test the equation of state of the dark energy  $w$  using the QSO power spectrum. This paper is organized as follows: In section 2, we describe our power spectrum analysis. In section 3, our theoretical modeling of the QSO power spectrum is explained. In section 4, constraint on the density parameters is discussed by fitting the 2QZ power spectrum. Section 5 is devoted to summary and conclusions. Throughout this paper we use the unit in which the light velocity equals 1.

## 2. The power spectrum analysis

In our power spectrum analysis, we use the complete sample of the full 2QZ survey, which is publicly available ([http://www.2dfquasar.org/Spec\\_Cat/](http://www.2dfquasar.org/Spec_Cat/)). The 2QZ survey covers two area of  $5 \times 75 \text{ deg}^2$ , one in the South Galactic Cap (SGC) and the other in the North Galactic

Cap (NGC), respectively, in the range of redshift less than 3. The survey area is defined by the equatorial coordinates from  $\alpha = 21^{\text{h}}40$  to  $\alpha = 3^{\text{h}}15$  and  $-32.5^\circ \leq \delta \leq -27.5^\circ$  in the SGC, and  $9^{\text{h}}50 \leq \alpha \leq 14^{\text{h}}50$  and  $-2.5^\circ \leq \delta \leq 2.5^\circ$  in the NGC, respectively. The survey area of the NGC is jagged and we select a simple rectangle area in our power spectrum analysis. Then we use 10713 and 8443 QSOs in the SGC and the NGC, respectively, in the range of redshift  $0.2 \leq z \leq 2.2$ <sup>1</sup>, incorporating the hole information publicly available.

We describe the estimator of the power spectrum adopted here. Three dimensional map is constructed by introducing the distance

$$s(z) = \int_0^z \frac{dz'}{H_0 \sqrt{0.3(1+z')^3 + 0.7}}, \quad (1)$$

where  $s$  is the comoving distance of the  $\Lambda$  cold dark matter model with the density parameter 0.3. We denote the density field by  $n(\mathbf{s})$  and the mean number density by  $\bar{n}(\mathbf{s})$ , where  $\mathbf{s} = s\boldsymbol{\gamma}$  with  $\boldsymbol{\gamma}$  specifying the direction. Introducing a random synthetic density field  $n_s(\mathbf{s})$ , which has mean number density  $1/\alpha$  times that of  $n(\mathbf{s})$ , we define the Fourier coefficient

$$\mathcal{F}(\mathbf{k}) = A^{-1/2} \int d\mathbf{s} [n(\mathbf{s}) - \alpha n_s(\mathbf{s})] e^{i\mathbf{k}\cdot\mathbf{s}} \quad (2)$$

with  $A = \int d\mathbf{s} \bar{n}(\mathbf{s})^2$ . The estimator of the power spectrum is defined

$$P(k) = \frac{1}{V_k} \int_{V_k} d\mathbf{k} |\mathcal{F}(\mathbf{k})|^2, \quad (3)$$

where  $V_k$  is the volume of a thin shell in the  $\mathbf{k}$ -space with the radius  $k$ . In the case  $\alpha \ll 1$ , the variance of the power spectrum is

$$\Delta P(k)^2 = \frac{2(2\pi)^3}{AV_k}. \quad (4)$$

Note that we have not used the optimal weighting scheme by setting the optimal weight factor being constant (Feldman, Kaiser and Peacock 1994, Tegmark et al. 1998, Yamamoto 2003b). This choice does not alter the result of the QSO power spectrum analysis because the QSO is sparse and  $\bar{n}P(k) < 1$ . Instead of equation (2), the discrete density field can be rephrased as

$$\mathcal{F}(\mathbf{k}) = A^{-1/2} \left[ \sum_i n(\mathbf{s}_i) e^{i\mathbf{k}\cdot\mathbf{s}_i} - \alpha \sum_j n_s(\mathbf{s}_j) e^{i\mathbf{k}\cdot\mathbf{s}_j} \right], \quad (5)$$

---

<sup>1</sup>The 2QZ group used the QSOs in the range of the redshift  $0.3 \leq z \leq 2.2$ , which is slightly different from our choice. This difference does not alter our result.

where  $\mathbf{s}_i$  and  $\mathbf{s}_j$  are the position of the  $i$ -th QSOs and the  $j$ -th random objects.

Figure 1 plots the power spectrum (filled squares), which is obtained by combining results from the SGC and NGC data sets. Fig.1 shows a good agreement with the result (open squares) by Outram et al. (2003). However, the error bar of our power spectrum is larger than that of 2QZ group. This can originate from the difference of the error estimator adopted, which we describe in more details below. The solid curve in Fig.1 is the theoretical curve of the  $\Lambda$  cold dark matter (CDM) model with the cosmological parameter,  $\Omega_m = 0.28$ ,  $\Omega_b = 0.045$ ,  $h = 0.7$ ,  $\sigma_8 = 0.9$  and  $n = 1$ , motivated by the WMAP result (Spergel et al. 2003, see also next section).

Finally in this section, we compare the error estimator of the power spectrum adopted in the present paper with that of the 2QZ group. There are two differences. First, they used the equation 2.3.2 in paper by Feldman et al. (1994). In the limit that  $\bar{n}$  is a constant, there is the discrepancy of the factor 2, if  $V_k$ , the volume of a thin shell in the  $\mathbf{k}$ -space, is same. In our analysis we used  $V_k = 4\pi k^2 \Delta k$ , where  $\Delta k$  is the width of the  $k$  bin. Our error estimator is consistent with that formulated by Tegmark et al. (1998; see equation 62 in their paper). Second, the 2QZ group adopted the different method for  $V_k$ , estimated by  $V_k = N_k(\Delta k)^3$  with  $N_k$  the number of independent modes in the  $k$ -shell and  $(\Delta k)^3$  the volume of one  $k$ -mode (for details see also Hoyle, et al. 2002; Hoyle 2000).

### 3. Modeling the theoretical power spectrum

The author considered a constraint on the density parameters,  $\Omega_m$  and  $\Omega_b$ , by fitting the 2dF QSO power spectrum found by Hoyle et al. (2002), in a previous investigation (Yamamoto 2002). We here adopt the similar methodology to apply it to the 2QZ power spectrum obtained in the previous section. The important improvement of the present work is the inclusion of nonlinear effects in modeling the theoretical power spectrum and a systematic uncertainty in measuring the redshift in the 2QZ survey, as well as the inclusion of an arbitrary equation of state parameter  $w$  of the dark energy. In this section we briefly explain the modeling, following the same notation in the previous paper.

We restrict ourselves to a spatially flat FRW universe and follow the quintessential cold dark matter (QCDM) model. The effective equation of state of the dark energy,  $w$ , can be a function of redshift, however, we consider the QCDM model with a constant equation of state for simplicity (Wang et al. 2000). In this case the relation between the comoving distance and the redshift is

$$r(z) = \frac{1}{H_0} \int_0^z \frac{dz'}{\sqrt{\Omega_m(1+z')^3 + (1-\Omega_m)(1+z')^{3(1+w)}}}, \quad (6)$$

where  $H_0 = 100h\text{km/s/Mpc}$  is the Hubble constant. Wang & Steinhardt (1998) have given a useful approximate formula for the linear growth index in the  $\Lambda\text{CDM}$  model, which we adopt in the present work. For nonlinear modeling of the mass density perturbation, we adopt the simple fitting formulae for the nonlinear mass perturbation power spectrum presented by Ma et al. (1999) for the  $\Lambda\text{CDM}$  model, combined with the transfer function by Eisenstein & Hu (1998), which is robust even when the baryon fraction is large.

To incorporate the nonlinear (Finger-of-God) effect due to the random motion of objects, we consider the power spectrum multiplied by the damping factor  $D[q_{\parallel}\sigma_{\text{P}}]$ , where  $\sigma_{\text{P}}$  is the pairwise velocity dispersion and  $q_{\parallel}$  is the comoving wave number parallel to the line-of-sight of an observer in real space. We adopt the expression assuming an exponential distribution function for the pairwise velocity, and the corresponding damping factor is (Mo, et al. 1997; Magira, et al. 2000)

$$D[q_{\parallel}\sigma_{\text{P}}] = \frac{1}{1 + q_{\parallel}^2\sigma_{\text{P}}^2/2}. \quad (7)$$

The pairwise velocity dispersion is the function of redshift  $z$ . We computed  $\sigma_{\text{P}}^2$  by the approximate formula for the mean square velocity dispersion at the large separation determined through the cosmic energy equation (Mo, et al. 1997; Magira, et al. 2000; Suto et al. 2000).

On the other hand, as described in the paper by Outram et al. (2003), systematic uncertainty in measurement of the redshift causes an apparent velocity dispersion. We incorporate the uncertainty in redshift-measurement  $\delta z$ , based on the following consideration. We write the density fluctuation field  $\delta(\mathbf{s})$  in a Fourier expansion form as

$$\delta(\mathbf{s}) = \sum_{\mathbf{k}} \delta_{\mathbf{k}} e^{i\mathbf{k}\cdot(\mathbf{s}+\Delta\mathbf{s})}, \quad (8)$$

where  $\Delta\mathbf{s}$  represents the error in measuring the position, which is related with  $\delta z$  by  $|\Delta\mathbf{s}| (= \Delta s) = \delta z(ds/dz)$ . Then an ensemble average of  $\delta(\mathbf{s})\delta(\mathbf{s}')$  can be written as

$$\langle \delta(\mathbf{s})\delta(\mathbf{s}') \rangle = \sum_{\mathbf{k}} \langle |\delta_{\mathbf{k}}|^2 \rangle e^{i\mathbf{k}\cdot(\mathbf{s}-\mathbf{s}')} \langle e^{i\mathbf{k}\cdot(\Delta\mathbf{s}-\Delta\mathbf{s}')} \rangle, \quad (9)$$

where we have assumed that  $\delta_{\mathbf{k}}$  and  $\Delta\mathbf{s}$  are independent probability variables and  $\langle \delta_{\mathbf{k}}\delta_{\mathbf{k}'} \rangle = \langle |\delta_{\mathbf{k}}|^2 \rangle \delta^{(3)}(\mathbf{k} - \mathbf{k}')$ . We further assume that the angular coordinates are well determined and  $\Delta\mathbf{s} = \gamma\Delta s$ . In this case, denoting the wave number of the line-of-sight direction by  $k_{\parallel}$ , we have

$$\langle e^{i\mathbf{k}\cdot(\Delta\mathbf{s}-\Delta\mathbf{s}')} \rangle = e^{-k_{\parallel}^2 \langle (\Delta s - \Delta s')^2 / 2 \rangle} = e^{-k_{\parallel}^2 \langle \Delta s^2 \rangle}, \quad (10)$$

where we have assumed that  $\Delta s$  and  $\Delta s'$  are independent Gaussian probability variables with the variance  $\langle \Delta s^2 \rangle$ . Therefore the damping factor due to the error in redshift-measurement is written

$$\mathcal{D}[\delta z] = \exp \left[ -k_{\parallel}^2 \left( \frac{ds}{dz} \right)^2 \langle \delta z^2 \rangle \right], \quad (11)$$

where  $\langle \delta z^2 \rangle$  is the variance of the error in measuring the redshift. In the present paper we adopt  $\delta z = 0.0027z$  following Croom et al. (2003). Figure 2 shows the damping factor  $D[k_{\parallel}\sigma_{\mathcal{P}}]$  (solid curves) in the  $\Lambda$ CDM model<sup>2</sup>, as function of the wave number  $k_{\parallel}$  with the redshift fixed as  $z = 0.5$ ,  $z = 1$  and  $z = 1.5$  for three curves from top to bottom. The dashed curves show the damping factor  $D[k_{\parallel}\sigma_{\mathcal{P}}]$  multiplied by  $\mathcal{D}[\delta z]$ . Because we are considering the angular averaged power spectrum, and this figure does not exactly express the damping factor of our power spectrum. However, this figure indicates that the damping factor have a substantial effect on the power spectrum shape. Thus the uncertainty in redshift-measurement can be an important factor in the power spectrum analysis.

Concerning the modeling of the bias, we assume the scale independent model. Following the previous work (Yamamoto 2002), we consider the model  $b(z) = b_0/D_1(z)^\nu$ , where  $b_0$  and  $\nu$  are the constant parameters and  $D_1(z)$  is the linear growth rate normalized as  $D_1(0) = 1$ . We determine  $b_0$  to minimize  $\chi^2$ , which we define in the next section. In the present paper, we show the result adopting  $\nu = 1$ . Our result slightly depends on  $\nu$ , however, plausible alternation of  $\nu$  does not alter our conclusion qualitatively. (see also Yamamoto 2002). We consistently use the number density per unit redshift per unit solid angle  $dN/dz$  from the catalogue.

It will be useful to show how the theoretical power spectrum depends on the equation of state  $w$  of the dark energy. Curves in Figure 3 are theoretical power spectra with the various equation of state  $w = -1$ (solid curve),  $w = -2/3$ (long dashed curve) and  $w = -1/3$ (dashed curve). The other cosmological parameter is fixed as  $\Omega_m = 0.28$ ,  $\Omega_b = 0.1$ ,  $h = 0.7$ ,  $\sigma_8 = 0.9$  and  $n = 1$ . The difference of the three curves comes from the geometric distortion effect: The comoving distance in real space is given by equation (6), while the power spectrum is measured in redshift space with the radial coordinate  $s(z)$  defined by equation (1). Therefore the power spectrum in redshift space is distorted compared with that in real space. Denoting the wave number in real space by  $q$ , the geometric distortion is described by the scaling of wave numbers  $q \rightarrow k/c$ , where  $c$  is the ratio  $dr/ds$  and  $r/s$  for the component parallel and perpendicular to the line-of-sight direction, respectively (for details see e.g., Ballinger et al.

---

<sup>2</sup>For definiteness,  $D[k_{\parallel}\sigma_{\mathcal{P}}]$  denotes the damping factor  $D[q_{\parallel}\sigma_{\mathcal{P}}]$  with replacing  $q_{\parallel}$  with  $(ds/dr)k_{\parallel}$ .

1996, Yamamoto 2002; 2003b). For the model with  $w > -1$ , the factor  $c$  becomes less than unity. This shifts the power spectrum from right (large  $k$ ) to left (small  $k$ ) for the model with  $w > -1$ , as is clearly shown in Fig. 3. Thus  $w$  can be measured from the redshift power spectrum due to the scaling effect of the geometric distortion. Such a test using the scaling effect is distinguished from the Alcock-Paczynski test which relies on the anisotropy of clustering in redshift space (e.g., Ryden 1995; Alcock & Paczynski 1979).

#### 4. Discussions

In this section we compare our observational power spectrum from the 2QZ catalogue with the theoretical model to constrain cosmological parameters. We introduce

$$\chi^2 = \sum_{i=1}^N \frac{[P^{\text{th}}(k_i) - P^{\text{ob}}(k_i)]^2}{\Delta P(k_i)^2}, \quad (12)$$

where  $P^{\text{th}}(k_i)$  is the value of the power spectrum from the theoretical model at the wave number  $k_i$ ,  $P^{\text{ob}}(k_i)$  is the observational data and  $\Delta P(k_i)$  is the variance of errors, for which we use the ( $N =$ )20 data points obtained in Fig. 1. Following the analysis by Outram et al. (2003), we consider the likelihood function  $\propto e^{-\chi^2/2}$ . Figure 4 shows contours of the likelihood function with  $\chi^2$  found when different values of the cosmological density parameters,  $\Omega_m$  and  $\Omega_b/\Omega_m$  are used in the theoretical modeling. Each panel corresponds to constraints for the difference model of  $P^{\text{th}}(k)$ : The panels (a), (c) and (d) assume  $w = -1, -2/3$  and  $-1/3$ , respectively. The panel (b) is same as (a), but switched off the damping factor due to the error in the redshift-measurement by setting  $\delta z = 0$  in equation (11). In Fig. 4, we fix the other parameters  $h = 0.7$ ,  $n = 1$  and  $\sigma_8 = 0.9$ . The curves are contours of confidence 65%, 95% and 99% on the plane.

First, the panel (b) in Fig. 4 shows the effect of the error in the redshift-measurement in modeling the power spectrum. The peak value of (a) is located at  $\Omega_m = 0.27$ , while that of (b) is located at  $\Omega_m = 0.24$ . Thus the effect of  $\delta z$  can be of importance for determining  $\Omega_m$ , precisely. Second, Fig. 4 demonstrates the constraint on the density parameters depends on the equation of state parameter  $w$  of the dark energy. It shows that the preferable value of  $\Omega_m$  and  $\Omega_b$  increases as  $w$  becomes large. Figure 5 shows the contour of the likelihood function with  $\chi^2$  found when different values of  $\Omega_m$  and  $w$  are used in the modeling the power spectrum, where we fixed  $\Omega_b = 0.045$ , motivated from the WMAP result (Spergel et al. 2003). It is shown that the density parameters in the range  $0.2 \lesssim \Omega_m \lesssim 0.4$  is preferable, which is not very sensitive to the value of  $w$ . Therefore the constraint on  $w$  is not very tight, and  $w \gtrsim -0.2$  ( $-0.1$ ) is only excluded at the one (two) sigma level.

## 5. Conclusion

In summary we have revisited the power spectrum analysis of the complete 2dF QSO sample, as a complementary test of the work by Outram et al. (2003). Our analysis has reproduced a power spectrum, which is consistent with the 2QZ group. We have investigated the fitting of the power spectrum including the light-cone effect, the geometric distortion and the nonlinear effects. It is shown that the QSO spatial power spectrum is consistent with the  $\Lambda$ CDM model with  $\Omega_m = 0.2 \sim 0.5$ , which is effectively consistent with the 2QZ group. However, our constraint is weaker than that of the 2QZ group. This will be traced back to the difference of the error estimation of the power spectrum. In the present paper, we have emphasized the importance of the error in measurement of the redshift  $\delta z$  because it may have influence in estimating the density parameters. We have also investigated the effect of the equation of state of the dark energy  $w$ . For models with large value of  $w > -1$ , the preferable value of the density parameters becomes large. When we fix the baryon density parameter as that found by the WMAP team, the matter density parameter  $0.2 \lesssim \Omega_m \lesssim 0.4$  is preferable. No tight constraint on  $w$  is obtained,  $w \gtrsim -0.2$  ( $-0.1$ ) is only excluded at the one (two) sigma level. In general QSO sample is sparse and the shot noise contribution is substantial. Therefore the constraint from it is not very tight. However, such a power spectrum analysis will provide more useful constraint on  $w$  when applied to the SDSS luminous red galaxy sample (Yamamoto 2003b) and next generation redshift survey such as the KAOS project (Seo and Eisenstein 2003).

The author thanks anonymous referee for useful comments on earlier version of the manuscript, which helped improve it. This work is supported in part by Grant-in-Aid for Scientific research of Japanese Ministry of Education, Culture, Sports, Science and Technology, No.15740155.



## REFERENCES

- Alcock, C., & Paczynski, B. 1979, *Nature*, 281, 358
- Ballinger, W. E., Peacock, J. A., & Heavens, A. F. 1996, *MNRAS*, 282, 877
- Calvao, M. O., de Mello Neto, J. R. T., & Waga, I. 2002, *Phys. Rev. Lett.* 88, 091302
- Croom, S. M., Shanks, T., Boyle, B. J., Smith, R.J., Miller, L., Loaring, N., & Hoyle, F. 2001, *MNRAS*, 325, 483
- Croom, S. M., Smith, R. J., Boyle, B. J., Shanks, T., Miller, L., Outram, P. J., & Loaring, N. S. 2003, preprint
- Eisenstein, D. J., & Hu, W. 1998, *ApJ*, 496, 605
- Feldman, H. A., Kaiser, N., & Peacock, J. A. 1994, *ApJ*, 426, 23
- Hoyle, F., 2000, PhD thesis, Univ. Durham
- Hoyle, F., Outram, P.J., Shanks, T., Croom, S.M., Boyle, B.J., Loaring, N., Miller, L., & Smith, R.J. 2002, *MNRAS*, 329, 336
- Ma, C.-P., Caldwell, R. R., Bode, P., & Wang, L. 1999, *ApJ*, 521, L1
- Matarrese, S., Coles, P., Lucchin, F., & Moscardini, L. 1997, *MNRAS*, 286, 115
- Matsubara, T., & Suto, Y. 1996, *ApJ*, 470, L1
- Matsubara, T., Suto, Y., & Szapdi, I. 1997, *ApJ*, 491, L1
- Magira, H., Jing, Y. P., & Suto, Y. 2000, *ApJ*, 528, 30
- Mo, J., Jing, Y. P., & Börner, G. 1997, *MNRAS*, 286, 979
- Nishioka, H., & Yamamoto, K. 1999, *ApJ*, 520, 426
- Outram, P.J., Hoyle, F., Shanks, T., Croom, S. M., Boyle, B. J., Miller, L., Smith, R. J., & Myers, A. D. 2003, *MNRAS*, 342, 483
- Ryden, B. S. 1995, *ApJ*, 452, 25
- Seo, H-J, & Eisenstein D. J. 2003, astro-ph/0307460
- Spiegel, D. N., et al. 2003, *ApJS*, 148, 175

- Suto, Y., Magira, H., Jing, Y. P., Matsubara, T., & Yamamoto, K. 2000, *Prog. Theor. Phys. Suppl.* 133, 183
- Tegmark, M., Hamilton, A. J. S., Strauss, M. A., Vogeley, & M. S., Szalay, A. S. 1998, *ApJ*, 499, 555
- Wang, L., Caldwell, R. R., Ostriker, J. P., & Steinhardt, P. J. 2000, *ApJ*, 530, 17
- Wang, L., & Steinhardt, P. J. 1998, *ApJ*, 508, 483
- Yamamoto, K., & Suto, Y. 1999, *ApJ*, 517, 1
- Yamamoto, K. 2002, *MNRAS*, 334, 958
- Yamamoto, K. 2003a, *MNRAS*, 341, 1199
- Yamamoto, K. 2003b, *ApJ*, 595, 577

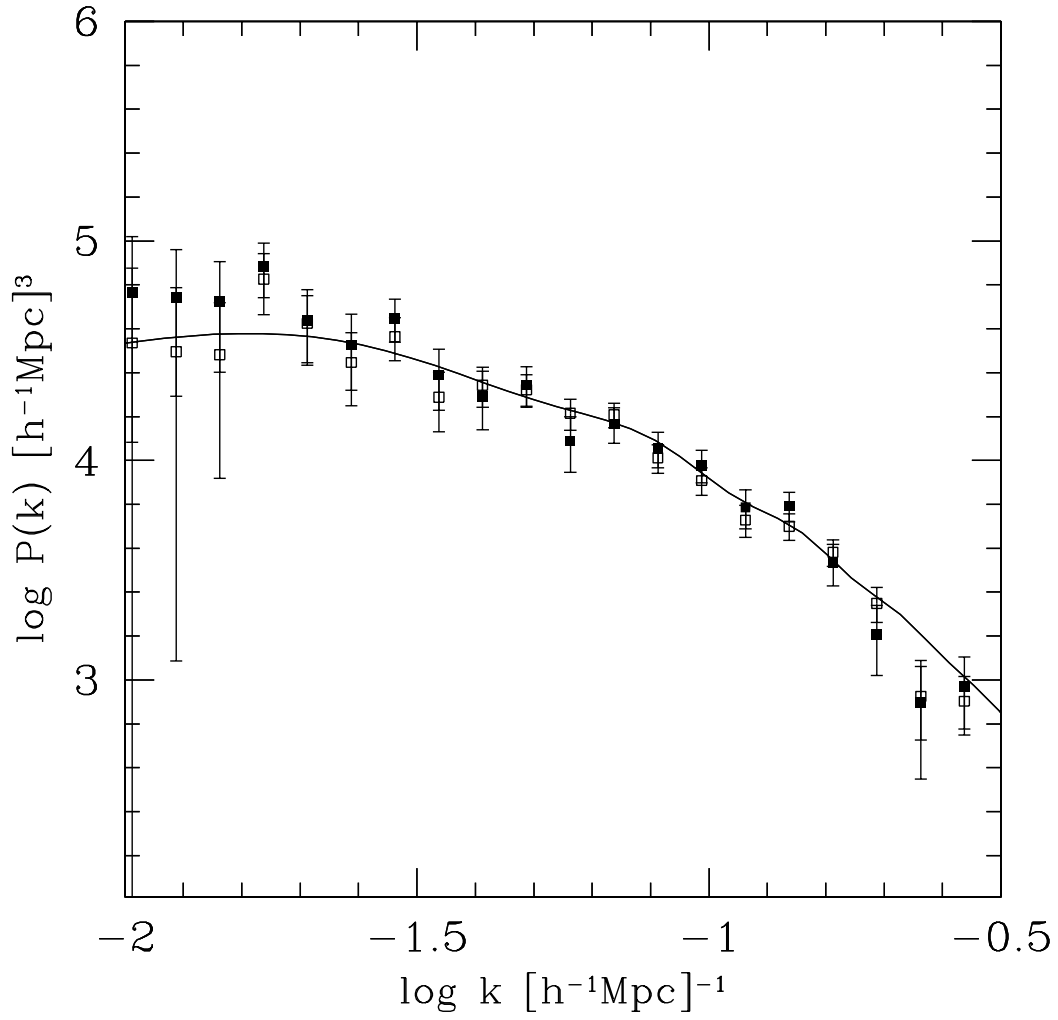


Fig. 1.— Power spectrum from the 2dF QSO sample. The filled square is the result of our analysis, while the open square is from Outram et al. (2003). The solid curve is the theoretical curve of the  $\Lambda$ CDM model with the cosmological parameter,  $\Omega_m = 0.28$ ,  $\Omega_b = 0.045$ ,  $h = 0.7$ ,  $\sigma_8 = 0.9$  and  $n = 1$ . (see also section 3)

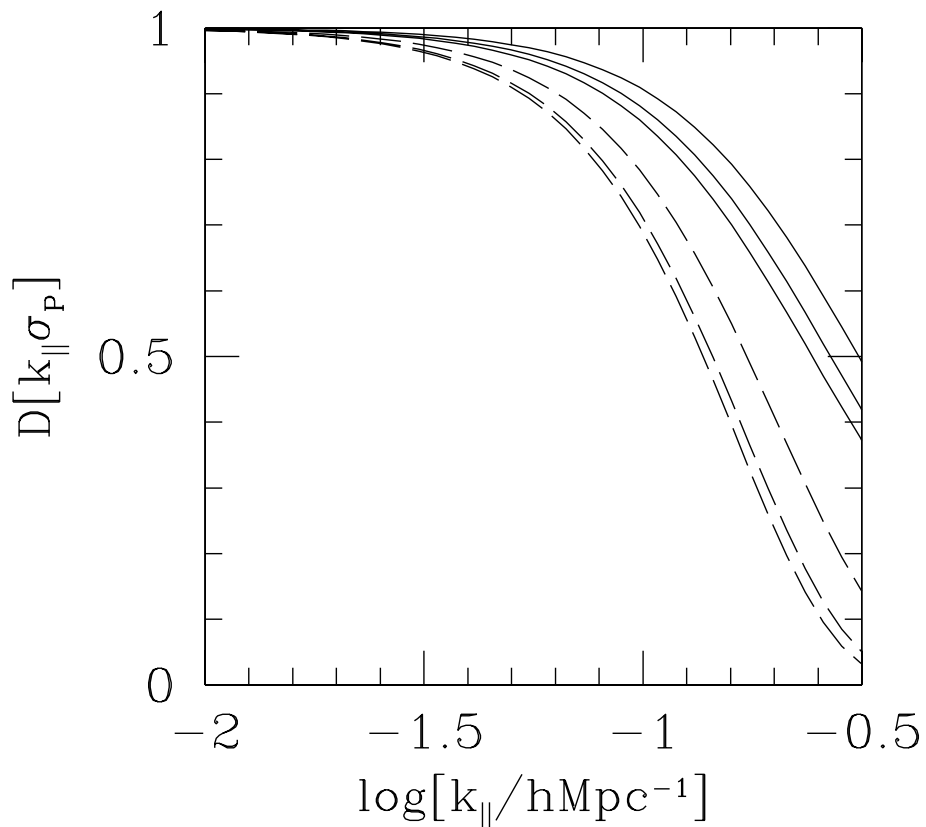


Fig. 2.— Damping factor  $D[k_{\parallel}\sigma_P(z)]$  (solid curves) as function of the wave number  $k_{\parallel}$  with the redshift fixed  $z = 0.5$ ,  $z = 1.0$  and  $z = 1.5$  from top to bottom. The dashed curves show the damping factor multiplied by  $\mathcal{D}[\delta z]$ . We assumed the same theoretical model as that in Fig. 1.

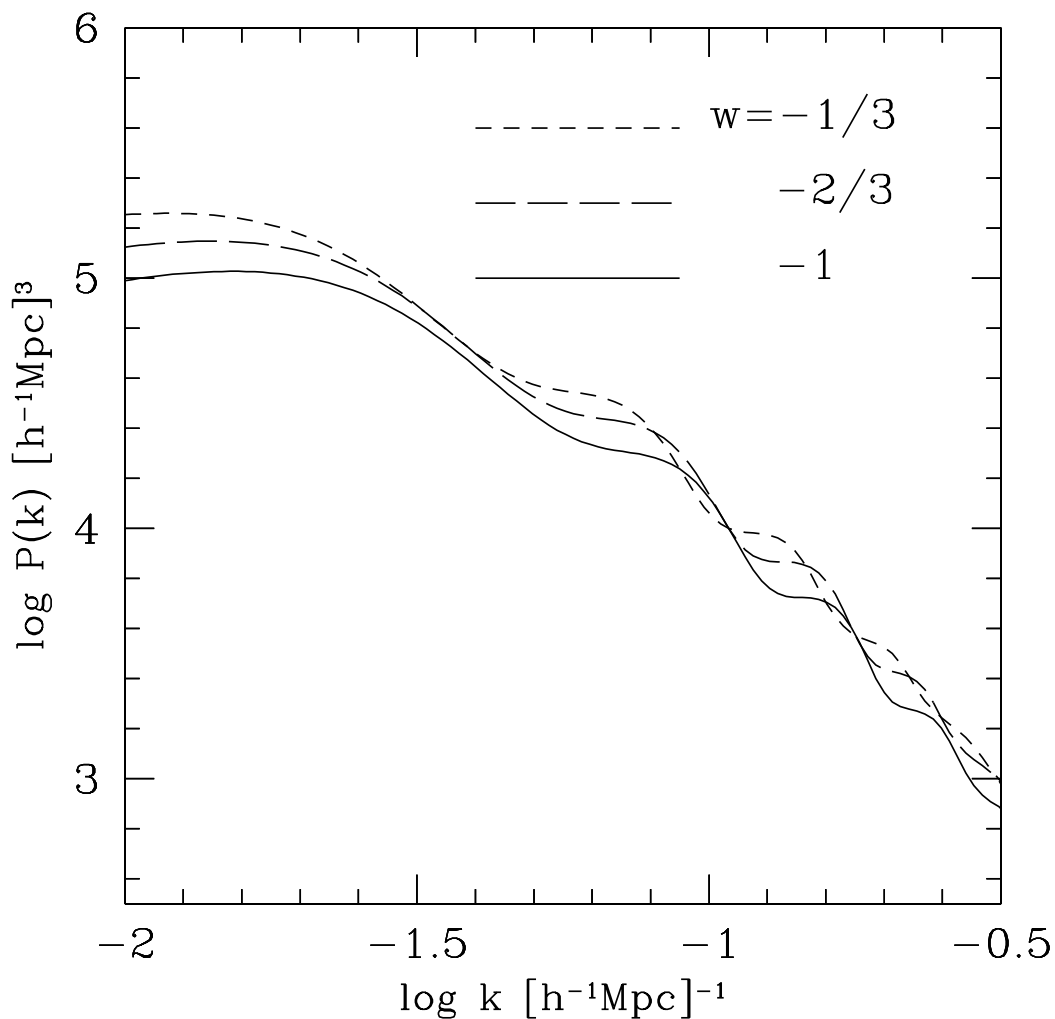


Fig. 3.— Theoretical power spectra with  $w = -1$  (solid curve),  $w = -2/3$  (long dashed curve) and  $w = -1/3$  (dashed curve). The other cosmological parameter is fixed as  $\Omega_m = 0.28$ ,  $\Omega_b = 0.1$ ,  $h = 0.7$ ,  $\sigma_8 = 0.9$  and  $n = 1$ . The amplitude is normalized as  $P(k) = 10^4 (h^{-1}\text{Mpc})^3$  at  $k = 0.1 h \text{Mpc}^{-1}$ . Note that the model of large baryon fraction is adopted to emphasize the scaling effect of the geometric distortion.

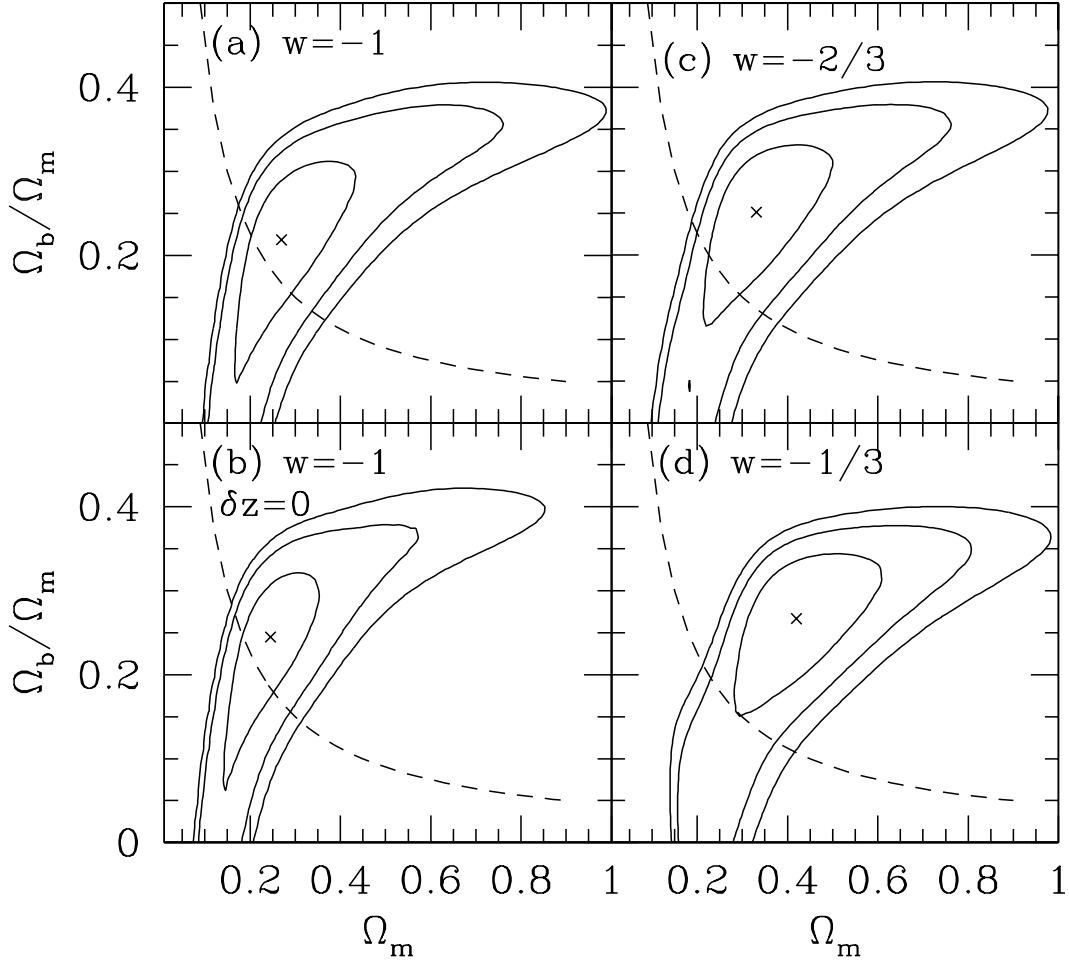


Fig. 4.— Contours of the likelihood function of our QSO power spectrum. The panel (a), (c) and (d) assumes  $w = -1$ ,  $-2/3$  and  $-1/3$ , respectively, in which we adopt  $h = 0.7$ ,  $n = 1$  and  $\sigma_8 = 0.9$ . The panel (b) is same as (a) but neglected the damping factor due to the error in redshift-measurement. In each panel, contours are confidence of 65%, 95% and 99%. The cross point shows the best fitted parameter:  $(\Omega_m, \Omega_b) = (0.27, 0.06)$ ,  $(0.24, 0.06)$ ,  $(0.33, 0.08)$ ,  $(0.41, 0.11)$ , from (a) to (d), respectively. The dashed curve shows  $\Omega_b = 0.045$  for comparison.

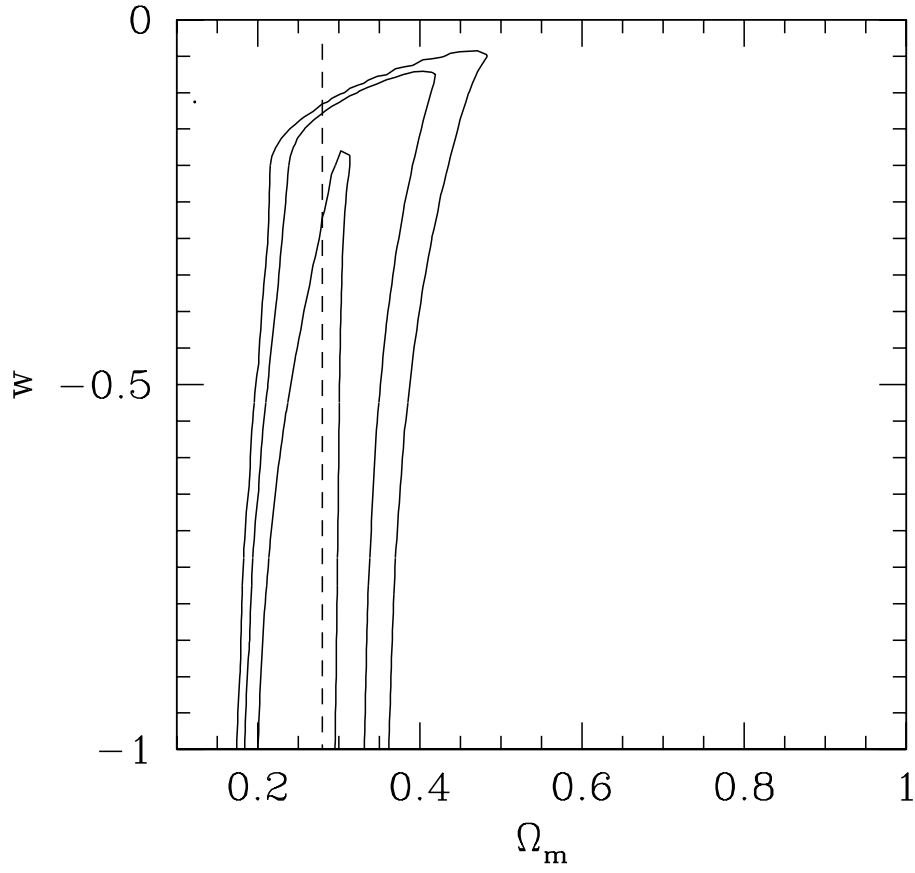


Fig. 5.— Contours of the likelihood function on the  $\Omega_m$  and  $w$  plane. Contours are confidence of 65%, 95% and 99%. Here we assume  $\Omega_b = 0.045$ ,  $h = 0.7$ ,  $n = 1$  and  $\sigma_8 = 0.9$ . The dashed line is  $\Omega_m = 0.28$ .